Journal of Theoretical Biology 264 (2010) 1214–1224

Contents lists available at ScienceDirect

Journal of Theoretical Biology

journal homepage: www.elsevier.com/locate/yjtbi

Compact energy metabolism model: Brain controlled energy supply

Britta Göbel [a], Dirk Langemann [b], Kerstin M. Oltmanns [c], Matthias Chung [d,*]

[a] Institute of Mathematics, Graduate School for Computing in Medicine and Life Sciences, University of Lübeck, Germany
[b] Institute Computational Mathematics, Technical University Braunschweig, Germany
[c] Department of Psychiatry and Psychotherapy, University of Lübeck, Germany
[d] Department of Mathematics and Computer Science, Emory University, Atlanta, USA

ARTICLE INFO

Article history:
Received 23 October 2009
Received in revised form
19 February 2010
Accepted 21 February 2010
Available online 15 March 2010

Keywords:
Energy metabolism
Glucose model
Dynamical system
Stability analysis
Model size reduction

ABSTRACT

The regulation of the energy metabolism is crucial to ensure the functionality of the entire organism. Deregulations may lead to severe pathologies such as obesity and type 2 diabetes mellitus. The decisive role of the brain as the active controller and heavy consumer in the complex whole body energy metabolism is the matter of recent research. Latest studies suggest that the brain's energy supply has the highest priority while all organs in the organism compete for the available energy resources. In our novel mathematical model, we address these new findings. We integrate energy fluxes and their control signals such as glucose fluxes, insulin signals as well as the ingestion momentum in our new dynamical system. As a novel characteristic, the hormone insulin is regarded as central feedback signal of the brain. Hereby, our model particularly contains the competition for energy between brain and body periphery. The analytical investigation of the presented dynamical system shows a stable long-term behavior of the entire energy metabolism while short time observations demonstrate the typical oscillating blood glucose variations as a consequence of food intake. Our simulation results demonstrate a realistic behavior even in situations like exercise or exhaustion, and key elements like the brain's preeminence are reflected. The presented dynamical system is a step towards a systemic understanding of the human energy metabolism and thus may shed light to defects causing diseases based on deregulations in the energy metabolism.

1. Introduction

The brain plays a decisive role in the regulation of the human whole body energy metabolism (Peters et al., 2004, 2007a, b). That motivates the investigation of the close link between cerebral energy supply and peripheral metabolic responses of the organism. We want to gain specific information about the regulatory elements of the brain in the human energy metabolism. In a novel approach, the human energy metabolism is mathematically modeled in a compact low-dimensional dynamical system so that the two central roles of the brain in the energy metabolism are addressed: first as a consumer and second as a superior administrative instance. The low-dimensional dynamical system models the integrative behavior of the whole body energy metabolism. The focussed compartments of course contain an enormous number of sub-systems from the biochemical via the molecular to the individual level. In the same manner, the interactions integrate tremendous amounts of relations, which are partly redundant. To our best knowledge, we for the first time include the brain as regulatory instance into such a mathematical model of the whole body energy metabolism. The purpose of our work is the development of a general model realistically describing the whole body energy metabolism in healthy humans.

Theoretical background of our work is the *selfish brain theory*, which provides a new approach to explain the regulation of the human whole body energy metabolism (Peters et al., 2004, 2007a, b). The selfish brain theory specifies mechanisms of the human brain to provide itself with adequate energy amounts while competing with the body periphery. Within this theory, the brain has two principal mechanisms to provide itself with sufficient energy, on the one hand the regulation of the appetite (ingestion) and on the other hand the allocation of energy resources from the body periphery. The brain is regarded as heavy energy consumer and superior regulatory instance and thus has the strongest position in the competition for energy within the body. The energy supply of the brain has the highest priority. Thus, identifying control mechanisms of the brain is a major goal to receive knowledge of pathological pathways and a systemic understanding of the human energy metabolism. For instance, recent clinical studies support the priority of the brain energy supply (Öz et al., 2009). Our novel model bases on physiological

* Corresponding author. Tel.: +1 404 727 7591; fax: +1 404 727 5611.
E-mail address: matthiaschung@gmail.com (M. Chung).
URL: http://www.mathcs.emory.edu/conrad (M. Chung).

0022-5193/$ - see front matter © 2010 Elsevier Ltd. All rights reserved.
doi:10.1016/j.jtbi.2010.02.033

pathways, energy sensing, and regulations discussed and specified in the review paper (Marty et al., 2007) and on controlling mechanisms of the brain investigated in Wang and Mariman (2008).

There exist various mathematical models describing interactions of the involved main determents of the human glucose metabolism. These models are based on the *glucostatic*, respectively, *lipostatic* theory, in which blood glucose or lipids are the regulated quantities (Kennedy, 1953; Mayer, 1953). Exemplarily, one could mention the well-known Minimal Model and the Ackerman Model (Ackerman, 1964; Bergman et al., 1981).

Nevertheless, recent mathematical models support central aspects of the selfish brain theory (Langemann, 2007; Langemann and Peters, 2008; Conrad et al., 2009). Furthermore, the impact of brain energy on pathological conditions such as ischemia is emphasized by means of detailed modeling and simulations of the brain energy metabolism by Vatov et al. (2006). Consequently, we see our novel model as a development of former mathematical models including the brain as major controller.

In Section 2, we present the mathematical model, which incorporates the central roles of the brain in the energy metabolism. The model considers five parts: the cerebral adenosine triphosphate (ATP; universal form of immediately available energy in every body cell), the energy in the body periphery in the form of glucose, glycogen, etc., blood glucose, insulin, and the ingestion regulation. In particular, it contains the competition for energy between brain and body periphery. The model describes the whole body energy metabolism on a short time scale with circadian ingestive behavior. Section 3 deals with the long-term effects in the energy metabolism. We discuss the transition to a middle-rate energy intake with its homeostatic energy levels and investigate the stability properties of the model. The model behavior is discussed in Section 4. A large class of influences on the energy metabolism can be modeled. We exemplarily demonstrate the scope of our new model by simulations of the energy metabolism at rest as well as upon exercise and exhaustion. We close our investigation with a general outlook and prospects of further exploration in Section 5.

2. Brain centered energy model

Conceptually, our model consists of two major components: on the one hand of energy fluxes between compartments and on the other hand of signals directing the energy fluxes within the organism. In our mathematical model, we consider the brain as consumer and more importantly as the superior administrative instance. In the following, we consider several energy metabolites, where A denotes the brain energy amount identified as ATP concentration, G is the blood glucose level, which is interpreted as blood glucose concentration, and R denotes the energy resources in the body (available energy reserves foremost in muscle/fat tissue, liver, and gastrointestinal tract in the form of glucose, glycogen, etc.). The model equations connect the time-derivatives of the energy levels with the energy fluxes

$$\dot{A} = \mathfrak{f}_{GA} - \mathfrak{u}_A, \tag{1a}$$

$$\dot{G} = -\mathfrak{f}_{GA} - \mathfrak{f}_{GR} + \mathfrak{f}_{RG}, \tag{1b}$$

$$\dot{R} = \mathfrak{f}_{GR} - \mathfrak{f}_{RG} + \mathfrak{f}_{in} - \mathfrak{u}_R. \tag{1c}$$

Here, $\mathfrak{f}_{GA}$ denotes the glucose flux from the blood into the brain across the blood brain barrier, $\mathfrak{f}_{GR}$ is the insulin dependent glucose flux from the blood into the energy stores and $\mathfrak{f}_{RG}$ is the flux from the energy resources into the blood. Food intake is modeled by the flux $\mathfrak{f}_{in}$, and it flows into the resource compartment since it comprises the gastrointestinal tract amongst others. Furthermore, the system contains the energy consumption of brain $\mathfrak{u}_A$ and periphery $\mathfrak{u}_R$. Hence, the need of the organism to consume energy is included in our model. Our model (1) bases on the conservation of energy. The only energy source in our model equations is $\mathfrak{f}_{in}$ whereas energy sinks are $\mathfrak{u}_A$, the energy consumption of the brain, and $\mathfrak{u}_R$, the energy consumption of muscle, fat, and others. Note, various types of energy, such as fat, glycogen, and glucose, are combined in the energy resources compartment R. Therefore, the energy consumption c_2 includes also the internal energy used to store and transform energy metabolites into other types of energy sources, e.g. biochemical processes of formation and mobilization of glycogen and fat/lipids. Moreover, since the energy resources compartment R includes the gastrointestinal tract, the energy intake model by $\mathfrak{f}_{in}$ directly appears in this compartment.

In addition to energy metabolites, our model contains control signals such as the plasma insulin concentration denoted by I and the ingestion of energy H. The signals I and H are described by the differential equations

$$\dot{I} = \mathfrak{s}_{AI} - \mathfrak{s}_I,$$

$$\dot{H} = \mathfrak{s}_{VH} - \mathfrak{s}_H.$$

The signal $\mathfrak{s}_{AI}$ describes the influence of the brain ATP level A on the insulin concentration I. In the following, the function V models the appetite and $\mathfrak{s}_{VH}$ the appetite dependent food intake. The signals $\mathfrak{s}_I$ and $\mathfrak{s}_H$ represent the self-inhibition of insulin secretion and ingestion, respectively.

The fluxes described above are forming a conceptual relation between compartments, signals, and energy fluxes within the organism. Next, we will specify the qualitative behavior of the fluxes and signals in our brain centered energy model. Generally, inductive influences are modeled as proportional relations and prohibitive influences are described by anti-proportional relations. This simplification catches the qualitative behavior, and it is able to model the quantitative behavior in the sense of a possible stationary point.

The glucose flux from the blood compartment into the brain crossing the blood brain barrier $\mathfrak{f}_{GA}$ is specified by facilitated diffusion intensified by a factor p_1 [M s^{-1}], i.e. $\mathfrak{f}_{GA} = p_1 G/A$. The smaller the actual cerebral ATP level A, the greater the flux is. Furthermore, glucose G needs to be available in the blood to cross the blood brain barrier. The glucose flux via the insulin dependent glucose transporter GLUT4 from the blood compartment into liver, muscle and fat tissue occurs if the blood glucose concentration G is high and the hormone insulin I is available in the blood at the same time. Hence, the insulin dependent glucose uptake from the blood into the stores is modeled by $\mathfrak{f}_{GR} = p_2 GI$ modulated by the parameter p_2 [(M s)$^{-1}$]. Our model combines energy resources and metabolites, such as lactate, glycerol, and glucogenic amino acids, in the compartment R. We assume glucose to be the only metabolite crossing the resources compartments R and the blood compartment G. Likewise, the energy flux from the resources into the blood compartment $\mathfrak{f}_{RG}$ is represented by facilitated diffusion proportional to the energy resources R and anti-proportional to the actual blood glucose concentration G with a factor p_3 [M s^{-1}], i.e. $\mathfrak{f}_{RG} = p_3 R/G$.

We assume the influx of energy into the resource compartment R to be proportional to the energy ingestion H with a factor p_6 [M s^{-1}], hence $\mathfrak{f}_{in} = p_6 H$. For now, our model assumes the energy consumption of the brain $\mathfrak{u}_A = c_1$ [M s^{-1}] and the energy consumption of the periphery $\mathfrak{u}_R = c_2$ [M s^{-1}] to be constant. In the following, $c := c_1 + c_2$ denotes the total energy consumption of the organism.

The hormone insulin acts not only as local response to the blood glucose concentration. Moreover, it is regarded as central

feedback signal of the brain $s_{AI} = p_4 A$ with an insulin secretion factor of the pancreatic β−cells p_4 [s^{-1}]. The brain may supply itself with energy by dropping the insulin concentration and therewith suppressing the glucose flux into the periphery (allocation mechanism). The degradation of insulin is supposed to be of first order $s_I = p_5 I$ with the insulin degradation rate p_5 [s^{-1}].

Low brain ATP A, insulin I, and blood glucose G cause appetite so that V anti-proportionally depends on brain ATP, blood glucose, and insulin amplified by a factor p_8 [M^3], i.e. $V = p_8/(AGI)$. We assume the signal onto the energy ingestion to be appetite dependent $s_{VH} = p_7 f(V)$ with a unitless parameter p_7. For once we abstract from the precise form of the ingestion activation function f and just assume f to be monotonously increasing in V and saturated. That means $f : [0,\infty) \to [0 f_{max}]$ with $f'(V) \geq 0$ for all V and $\lim_{V\to\infty} f(V) = f_{max}$. Furthermore, the assumption of at most one inflection point seems natural, and we get $f'(V) > 0$ for all V with $0 < f(V) < f_{max}$. Since we have in mind that a small appetite induces a nearly vanishing ingestion, we call a function f fulfilling these conditions sigmoidal. Furthermore, we suppose the energy ingestion to be subject to a self-inhibition $s_H = p_7 H$.

Thus, our novel model of the energy metabolism is given by the system of the five ordinary differential equations

$$\dot{A} = p_1 \frac{G}{A} - c_1, \tag{2a}$$

$$\dot{G} = -p_1 \frac{G}{A} - p_2 GI + p_3 \frac{R}{G}, \tag{2b}$$

$$\dot{I} = p_4 A - p_5 I, \tag{2c}$$

$$\dot{R} = p_2 GI - p_3 \frac{R}{G} + p_6 H - c_2, \tag{2d}$$

$$\dot{H} = p_7 (f(V) - H) \tag{2e}$$

with

$$V = \frac{p_8}{AGI}. \tag{2f}$$

All functions A, G, I, R, H, and V are functions in time t and are assumed to be positive. Likewise, the model parameters $p_1, \ldots, p_8$ and c_1,c_2 are supposed to be positive. Fig. 1 visualizes the different fluxes and signals of model (2).

Describing fluxes by quotients of quantities is fairly uncommon. The linear approach is more prevalent in which fluxes are modeled by differences of quantities. This can be seen as passive diffusion process. However, since we are interested in controlled diffusion processes, we model fluxes by quotients of quantities. For instance, the flux $f_{GA} = p_1 G/A$ in Eq. (2a) is controlled by the brain compartment. Suppose the cerebral energy level A is low, the diffusion process from the blood compartment into the brain is accelerated by the low energy level in the brain compartment. Contrary, high levels of A inhibit the diffusion process into the brain.

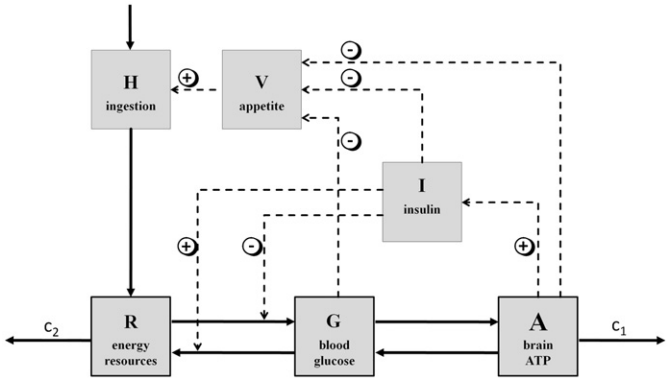

Fig. 1. Energy fluxes between compartments (solid) and control signals directing the energy fluxes in the organism (dashed). Energy supply chain of periphery R, blood glucose G, and brain ATP A. The ingested energy H passes resources R and blood G and is transported into the brain as final consumer. Energy is consumed by the brain (c_1) and the periphery (c_2). While the appetite V (affected by A, G, and I) controls the ingestion H, insulin I additionally controls the allocation to the brain via control of the blood glucose flux.

We get a first insight into the overall behavior of the energy fluxes and the energy related signals by two simple mind games. First, suppose that the brain ATP concentration A decreases below an "adequate" level (compare Fig. 2(a)). This has a direct impact on the alteration of blood glucose G and insulin I. Since A decreases the positive stimulus on the insulin secretion $p_4 A$ drops and the insulin level will decrease. By this, the brain reduces the blood glucose uptake into the peripheral tissue $p_2 G I$ and allocates itself energy. Furthermore, the change in A has some impact on the blood glucose level G in three more ways. First, the blood glucose compartment deals with an increased flux to the brain via $p_1 G/A$ (increased blood pressure, permeability of the blood brain barrier). Second, the energy resources of the body are increasingly tapped by $p_3 R/G$ (increases glucagon and therefore causing the liver to convert stored glycogen into glucose), and thirdly the blood glucose G is prevented to drift and to be stored into the muscle and fat tissue via $p_2 GI$. This effect is amplified by the mentioned reduction of insulin I. The decrease of blood glucose G is only prevented by the flux of energy from the resources R into the blood stream. While not "sufficient" energy is ingested (positive stimulus via $p_6 H$), the energy resources R (glycogen, energy substrates from the digestive tract, muscle, fat tissue, and liver) decrease, blood glucose G is further reduced, and the brain ATP concentration A is threatened to drop even more. Thus, if the energy resources R are depleted, only the ingestion of energy H may provide the required energy for the entire organism. Since A, G, and I are reduced, the appetite defined by $V = p_8/(AGI)$ increases. In case the appetite V exceeds a certain limit $f(V) > H$ (f is a strictly monotonously increasing function), the organism will ingest nutrients. By this, the organism is protected from running out of energy. This is a first verbal explanation for model (2) ensures that the brain as the hierarchical highest organ is sufficiently supplied with energy.

Second, we discuss the brain ATP level A to be elevated above a "normal" level (compare Fig. 2(b)). The energy flux to the brain decreases via $p_1 G/A$ (reduced blood pressure, less permeable blood brain barrier). In the same line, insulin is synthesized via $p_4 A$ to enable blood glucose to enter liver, muscle and fat tissue via its GLUT4 receptors ($p_2 GI$). Hence, the organism stores glucose in the peripheral energy resources R.

The considerations above give a first insight into the behavior of model (2). We verify the argumentations by investigations and simulations in the following. Further analysis on the qualitative behavior will be presented in the following sections.

3. Model analysis

3.1. Scaling

Our model (2) consists of eight parameters p_j, $j = 1,\ldots,8$, and the energy consumptions c_1, c_2. All these parameters contain quantitative physiological information. By rescaling we will be able to reduce the complexity of eight down to five parameters while maintaining the behavior of our model, merely changing the scales. We set

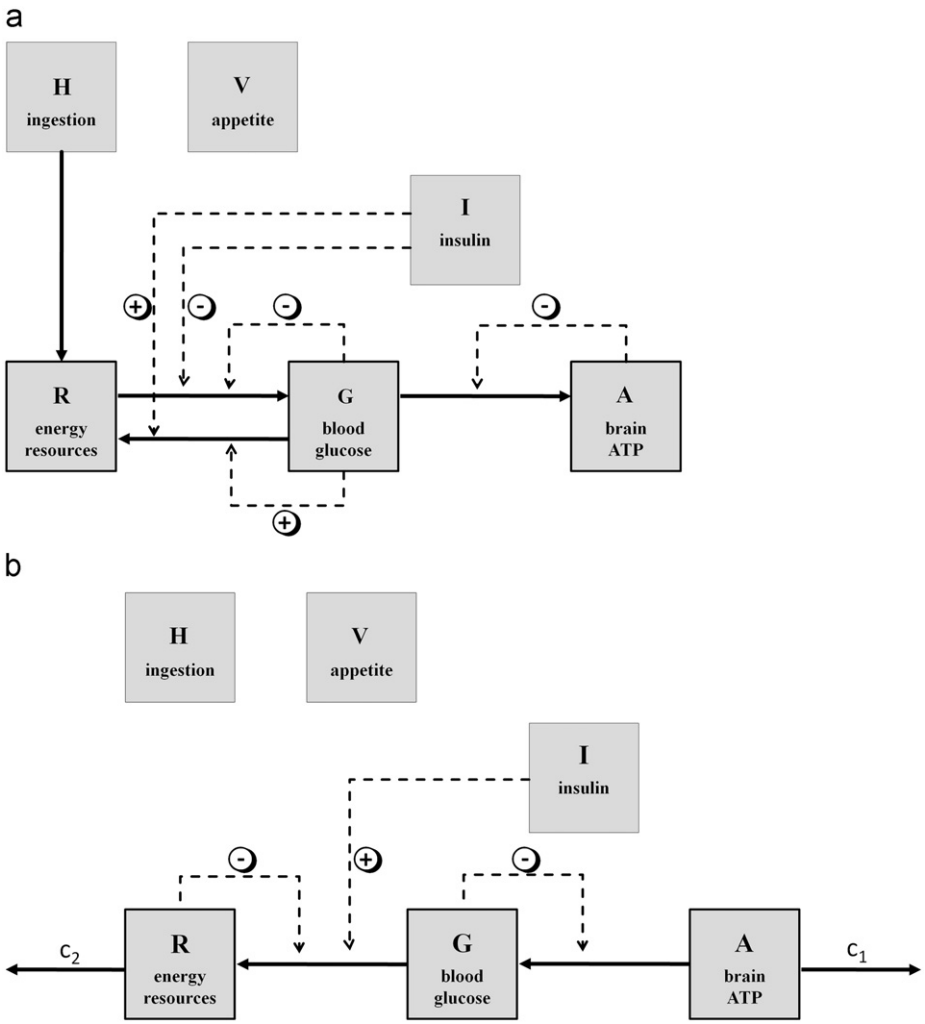

Fig. 2. Energy flux in the organism. Figure (a) shows the energy supply chain in case of low brain ATP A. Beside a flux from the blood glucose G towards the energy resources R controlled by insulin I, all others flow toward the brain compartment A, which therefore symbolizes the highest hierarchical level in energy supply. Figure (b) shows the energy efflux and inhibition of the system. This situation occurs in case of high brain ATP A. The energy mainly flows from the brain into peripheral energy stores R.

$$A=\alpha A',\quad G=\gamma G',\quad I=\imath I',\quad R=\varrho R',\quad H=\eta H',\quad t=t'/\tau,$$

with $\alpha=\gamma=\varrho$ and

$$\tau=p_5,\quad \alpha=\frac{p_1}{\tau},\quad \imath=\frac{\tau}{p_2},\quad \eta=\frac{\tau\alpha}{p_6},$$

and we denote new quantities

$$c_1'=\frac{c_1}{p_1},\quad c_2'=\frac{c_2}{p_1},\quad p_3'=\frac{p_3}{p_1},\quad p_4'=\frac{p_4\alpha}{p_2},$$
$$p_6'=\frac{p_6}{p_1},\quad p_7'=\frac{p_7}{p_5},\quad p_8'=\frac{p_8}{\alpha^2\imath}.$$

We now replace $X'\to X$ for $X\in\{A,G,I,R,H,c_1,c_2,p_3,p_4,p_6,p_7,p_8\}$, and the scaled dynamical system reads

$$\dot A=\frac{G}{A}-c_1, \tag{3a}$$

$$\dot G=-\frac{G}{A}-GI+p_3\frac{R}{G}, \tag{3b}$$

$$\dot I=p_4A-I, \tag{3c}$$

$$\dot R=GI-p_3\frac{R}{G}+H-c_2, \tag{3d}$$

$$\dot H=p_7(p_6f(V)-H), \tag{3e}$$

with

$$V=\frac{p_8}{AGI}, \tag{3f}$$

with the five parameters p_3, p_4, p_6, p_7, and p_8.

3.2. Transition for increasing ingestion sensitivity

The parameter p_7 reflects the sensitivity of the organism in ingesting nutrition consistent with its need for energy. A low value of p_7 indicates a slow adaption to the body's energy needs while a rather high value corresponds to a fast adaption of the body's energy needs. For further increasing p_7 the ingestion is strongly regulated so that the energy uptake immediately satisfies the needs of the organism.

Let us consider a system of the form

$$\dot x=\phi(x,y),\quad x(0)=x_0\in\mathbb{R}^{d-1}, \tag{4a}$$

$$\dot y=k(\psi(x)-y),\quad y(0)=y_0\in\mathbb{R}, \tag{4b}$$

with sufficient smooth functions $\phi:\mathbb{R}^{d-1}\times\mathbb{R}\to\mathbb{R}^{d-1}$, $\psi:\mathbb{R}^{d-1}\to\mathbb{R}$ and a parameter $k>0$. We show that the solution $x(t)$ tends to the solution of a lower-dimensional system for increasing k.

Theorem 3.1. *If the function ϕ is Lipschitz-continuous with respect to the second variable y, then the solution of system (4) fulfills*

$$\lim_{k\to\infty} y(t) = \psi(x(t)) \tag{5}$$

for every fixed time instant t and the limit

$$\lim_{k\to\infty} x(t) = u(t) \tag{6}$$

is a solution of the differential equation $\dot{u} = \phi(u,\psi(u))$.

Proof. The second equation of system (4) is the inhomogeneous linear differential equation $\dot{y} + ky = k\psi(x)$ with the solution

$$\begin{aligned} y(t) &= y_0 e^{-kt} + k\int_0^t e^{k(\tau-t)}\psi(x(\tau))\,d\tau \\ &= y_0 e^{-kt} + \psi(x(\tau_1))\int_0^{t-\varepsilon} ke^{k(\tau-t)}\,d\tau + \psi(x(\tau_2))\int_{t-\varepsilon}^{t} ke^{k(\tau-t)}\,d\tau, \end{aligned}$$

with some $\tau_1 \in [0,t-\varepsilon)$ and $\tau_2 \in (t-\varepsilon,t)$ for every $\varepsilon \in (0,t)$. Now, it holds

$$\lim_{k\to\infty}\int_0^{t-\varepsilon} ke^{k(\tau-t)}\,d\tau = 0, \quad \lim_{k\to\infty}\int_{t-\varepsilon}^{t} ke^{k(\tau-t)}\,d\tau = 1$$

and hence

$$\lim_{k\to\infty} y(t) = \psi(x(\tau_2)),$$

with a $\tau_2 \in (t-\varepsilon,t)$ for every small $\varepsilon > 0$. The transition $\varepsilon \to 0$ yields the required result (5). Since the function ϕ is Lipschitz-continuous with respect to y, it holds true that a disturbance in the parameter y bounds the disturbance in the solution x for every fixed time instant t, thus (6) holds (Walter, 1970). □

Performing this procedure on the dynamical system (3) with $x = (A,G,I,R)^\top$, $y = H$, $\psi = p_6 f$, and p_7 in the role of k, the transition with an increasingly strong regulation of H, i.e. $p_7 \to \infty$, leads to the lower dimensional system of differential equations

$$\dot{A} = \frac{G}{A} - c_1, \tag{7a}$$

$$\dot{G} = -\frac{G}{A} - GI + p_3\frac{R}{G}, \tag{7b}$$

$$\dot{I} = p_4 A - I, \tag{7c}$$

$$\dot{R} = GI - p_3\frac{R}{G} + p_6 f\left(\frac{p_8}{AGI}\right) - c_2, \tag{7d}$$

with the four parameters p_3, p_4, p_6, and p_8. With the dynamical system (7) we obtained a description of the human whole body energy metabolism on a long time scale by regarding the mean ingestion of energy. In system (3), the ingestion is dynamically regulated, and it may oscillate around $p_6 f(V)$ on a short time scale. On a long time scale, the oscillation is negligible, and the mean regulation of H to $p_6 f(V)$ becomes more and more important. Thus, system (7) generated by $p_7 \to \infty$ can be regarded as long-term model of the human energy metabolism.

3.3. Stability analysis

This subsection deals with existence and uniqueness of stationary points, and we investigate their stability behavior.

Proposition 3.2. *If $c < p_6 f_{\max}$ holds true, then the system of differential equations (3) has exactly one stationary point $(A_\infty,G_\infty,I_\infty,R_\infty,H_\infty)^\top$.*

Proof. With the stationary condition $\dot{A} = \dot{G} = \dot{I} = \dot{R} = \dot{H} = 0$, we get

$$H_\infty = c = c_1 + c_2$$

by adding (3a), (3b), and (3d). Eq. (3e) yields $p_6 f(V_\infty) = c$. Due to the preconditions, we find a unique $V_\infty = f^{-1}(c/p_6)$. From Eqs. (3a) and (3c), we know

$$G_\infty = c_1 A_\infty \quad \text{and} \quad I_\infty = p_4 A_\infty.$$

Due to Eq. (3f), it holds true $A_\infty G_\infty I_\infty = p_8/V_\infty$, what leads to

$$A_\infty = \sqrt[3]{\frac{p_8}{c_1 p_4 V_\infty}} = \sqrt[3]{\frac{p_8}{c_1 p_4 f^{-1}(c/p_6)}}.$$

Finally, Eq. (3b) provides

$$R_\infty = \frac{c_1^2 A_\infty}{p_3}(1 + p_4 A_\infty^2).$$

Thus, the stationary condition has lead to a single stationary point. □

Proposition 3.3. *If $c < p_6 f_{\max}$ holds true, then the system of differential equations (7a) has the unique stationary point*

$$(A_\infty,G_\infty,I_\infty,R_\infty)^\top = \left(\sqrt[3]{\frac{p_8}{c_1 p_4 f^{-1}(c/p_6)}}, c_1 A_\infty, p_4 A_\infty, \frac{c_1^2 A_\infty}{p_3}(1 + p_4 A_\infty^2)\right)^\top.$$

Proof. The proof is done by straightforward calculation starting with system (7). □

Hence, the stationary point of system (7) is a projection of the stationary point of system (3). Thus, both stationary points coincide in the occurring quantities. The condition $c < p_6 f_{\max}$ is metabolically reasonable because the ability to ingest the consumed energy is a necessary condition for the existence of stationary states of the organism.

Theorem 3.4 will give inside to the long-term behavior of our model.

Theorem 3.4. *In the case $p_6 f(V) = V$ and on conditions*

$$\frac{p_8}{p_4} \le c_1 c, \tag{8a}$$

$$c_1 c \le p_4 p_8 \quad \text{if } c_1 \le 1, \tag{8b}$$

$$c_1^2 c \le p_4 p_8 \quad \text{if } c_1 > 1, \tag{8c}$$

$$c_1^2 \le p_3, \tag{8d}$$

the stationary point $(A_\infty,G_\infty,I_\infty,R_\infty)^\top$ of system (7) is asymptotically stable.

Proof. The Jacobian of the dynamical system (7) is given by

$$J = \begin{pmatrix} -\frac{G}{A^2} & \frac{1}{A} & 0 & 0 \\ \frac{G}{A^2} & -\frac{1}{A} - I - \frac{p_3 R}{G^2} & -G & \frac{p_3}{G} \\ p_4 & 0 & -1 & 0 \\ g'GI & I + \frac{p_3 R}{G^2} + g'AI & G + g'AG & -\frac{p_3}{G} \end{pmatrix},$$

with $g(C) = p_8/C$, $g'(C) = -p_8/C^2$, and $C = AGI$, $C > 0$. Since $G_\infty = c_1 A_\infty$, $I_\infty = p_4 A_\infty$, and $p_3 R_\infty / G_\infty^2 = p_4 A_\infty + 1/A_\infty$, the Jacobian

in the stationary point $(A_\infty,G_\infty,I_\infty,R_\infty)^\top$ reads

$$J_\infty = \begin{pmatrix} -\frac{c_1}{A_\infty} & \frac{1}{A_\infty} & 0 & 0 \\ \frac{c_1}{A_\infty} & -\frac{2}{A_\infty}-2p_4A_\infty & -c_1A_\infty & \frac{p_3}{c_1A_\infty} \\ p_4 & 0 & -1 & 0 \\ p_4c_1g'A_\infty^2 & 2p_4A_\infty+\frac{1}{A_\infty}+p_4g'A_\infty^2 & c_1A_\infty(1+g'A_\infty) & -\frac{p_3}{c_1A_\infty} \end{pmatrix}.$$

We will show that J_∞ has eigenvalues with negative real parts only (see Appendix A for details on calculation). The characteristic polynomial reads

$$\det(J_\infty-\lambda E)=a_4\lambda^4+a_3\lambda^3+a_2\lambda^2+a_1\lambda+a_0. \tag{9}$$

Since $g'(C)<0$ holds, the coefficients $a_0,\ldots,a_4$ are positive for all parameters, i.e. the necessary condition for negative real parts holds true.

Following the Hurwitz criterion, we investigate the minors $\mathcal{H}_1,\mathcal{H}_2,\mathcal{H}_3$, and $\mathcal{H}_4$ of the Hurwitz determinantes (Khalil, 2002). It holds $\mathcal{H}_1=a_3>0$ and since $\mathcal{H}_4=a_0\mathcal{H}_3$ it determines $\mathcal{H}_4>0$ if and only if $\mathcal{H}_3>0$. Therefore, we have to investigate the positivity of the critical terms $\mathcal{H}_2$ and $\mathcal{H}_3$. As the minor $\mathcal{H}_2$ is linear in $g'(C)$ and $\mathcal{H}_3$ is quadratic in $g'(C)$, we get with Taylor expansions

$$\mathcal{H}_2(g'(C))=a_3a_2-a_4a_1=\mathcal{H}_2(0)+g'(C)\cdot\mathcal{H}_2'(0)$$

and

$$\mathcal{H}_3(g'(C))=a_1a_2a_3-a_0a_3^2-a_1^2a_4=\mathcal{H}_3(0)+g'(C)\cdot\mathcal{H}_3'(0)+1/2(g'(C))^2\cdot\mathcal{H}_3''(0).$$

Since $\mathcal{H}_2(0)$ and $\mathcal{H}_3(0)$ are constructed by positive terms only, it follows $\mathcal{H}_2(0)>0$ and $\mathcal{H}_3(0)>0$. Thus, sufficient small $|g'(C)|$ always assures stability. Since $g'(C)<0$ holds, the condition $\mathcal{H}_2'(0)<0$ leads to $\mathcal{H}_2(g'(C))>0$ for all $g'(C)$. Inequality (8d) provides $\mathcal{H}_2'(0)<0$. Condition (8a) implies $A_\infty<1$. If additionally inequality (8b) respectively (8c) is satisfied, the negative summands of $\mathcal{H}_3'(0)$ dominate the positive summands of $\mathcal{H}_3'(0)$ and therefore $\mathcal{H}_3'(0)<0$. Finally, the condition $\mathcal{H}_2'(0)<0$ assures $\mathcal{H}_3''(0)>0$, which proves the asymptotical stability of the stationary point $(A_\infty,G_\infty,I_\infty,R_\infty)^\top$. □

Remark. The conditions (8) are sufficient but not necessary. The parameter set leading to an asymptotical stable system behavior is larger.

In other words, provided the inequalities (8) are satisfied, the solution of the system of differential equations (7) settles to a set-point over time. This implies that the system is in a homeostatic state if we regard the mean ingestion of energy. How may the conditions (8) now be construed?

The inequalities (8a)–(8c) provide a lower, respectively, upper bound for the energy consumptions c_1 and c_2. These bounds depend on allocation p_4 as well as on appetite p_8. This implies that the brain's pathways of energy supply restrict the total energy consumption of the organism. The ratio of appetite and allocation provides the lower bound indicating that the brain first tries to provide energy via allocation. The product of allocation and appetite is the upper bound. Furthermore, from a physiological point of view inequality (8d) holds if the energy release from the stores into the blood p_3 dominates the cerebral energy consumption c_1.

Remark. If $\mathcal{H}_2'(0)$ or $\mathcal{H}_3'(0)$ is positive, one of the stability conditions (8) is not satisfied, wherefore we need a restriction on $g'(C)$, i.e. sufficient small $|g'(C)|$, to receive stability. Unstable situations occur for very large $|g'(C)|$ and positive $\mathcal{H}_2'(0)$ or $\mathcal{H}_3'(0)$.

Remark. Theorem 3.4 gives stability conditions for the scaled parameters in Section 3.1. For the non-scaled parameters the stability conditions read

$$\frac{p_2^2p_5^2p_8}{p_1p_4}\le c_1c, \tag{10a}$$

$$\frac{c_1c}{p_1}\le p_4p_8,\quad \text{if } c_1\le p_1, \tag{10b}$$

$$\frac{c_1^2c}{p_1^2}\le p_4p_8,\quad \text{if } c_1>p_1, \tag{10c}$$

$$\frac{c_1^2}{p_1}\le p_3. \tag{10d}$$

Remark. System (3) features an instable stationary point implying that oscillating behavior may occur.

4. Simulation results

In this section, we examine the behavior of our model (2) including the ingestion dynamic. We simulate the human whole body energy metabolism at rest and the effects on the energy metabolism during exercise and exhaustion. These interventions influence the energy consumption of the organism modeled by time dependent functions $c_1(t)$ and $c_2(t)$. Since we are additionally interested in the long-term behavior of our metabolism model, we examine our long-term model (7). In order to obtain physiological values we refer our simulations to the non-scaled models (2) and (12). Here, (12) is the non-scaled reading of the long-term model (7). It can be derived by equivalent calculations of Section 3.1.

Exemplarily, we use the monotonously increasing function

$$f(V)=\frac{1}{2}+\frac{1}{\pi}\arctan\left(\frac{V-p_9}{p_{10}}\right) \tag{11}$$

describing the stimulus on food intake depending on appetite V. Here, the unitless parameter p_9 gives a loose intake threshold while p_{10}, which is unitless as well, controls the sensitivity of the ingestion stimulus. Since $f(V)\in[0,1]$, the ingestion is modeled with maximal intake for $f(V)=1$ and no uptake for $f(V)=0$.

As derived in Section 2 each parameter in our model (2) has a physiological interpretation. Rough estimates of our model parameters $p_1,\ldots,p_5$ and c_1,c_2 can be derived from the literature. The parameters $p_6,\ldots,p_{10}$ are related to ingestion and estimates are harder to quantify.

We choose $p_1\approx0.004\,\text{mM/s}$ for the glucose diffusion rate across the blood brain barrier (Tsuji, 2005). Baron and Clark (1997) quantify the insulin dependent whole body glucose uptake with 0.06 mM/s. This corresponds to $p_2\approx0.00013\,(\text{pMs})^{-1}$. (Flakoll et al., 1992) specify the amount of glucose stored in the body per time unit ($p_3\approx0.01\,\text{mM/s}$). For the insulin secretion rate we choose $p_4\approx5.7\,\text{s}^{-1}$, see Simon et al. (2000), and information about insulin clearance can be found in Fugleberg et al. (1982) ($p_5\approx7.1\,\text{s}^{-1}$). Flakoll et al. (1992) specify the maximal rate of glucose utilization ($c\approx0.07\,\text{mM/s}$), which provides an insight into the peripheral energy consumption c_2 and the cerebral energy consumption c_1, since the brain uses about 25% of the total body glucose utilization (Clark and Sokoloff, 1999). Starting with these rough approximates we performed an parameter estimation to identify a parameter set, which reflects the typical daily profiles of plasma glucose, insulin, and ATP levels (compare Day et al., 2003; Ainscow et al., 2002). The identified parameter values $p=(p_j)_{j=1}^{10}=(0.001,0.0001,0.03,5.8,0.04,50,0.005,1800,3.1,0.00005)^\top$ and $c_1=0.005$, $c_2=0.025$ replicate a healthy organism as illustrated in Figs. 3–6.

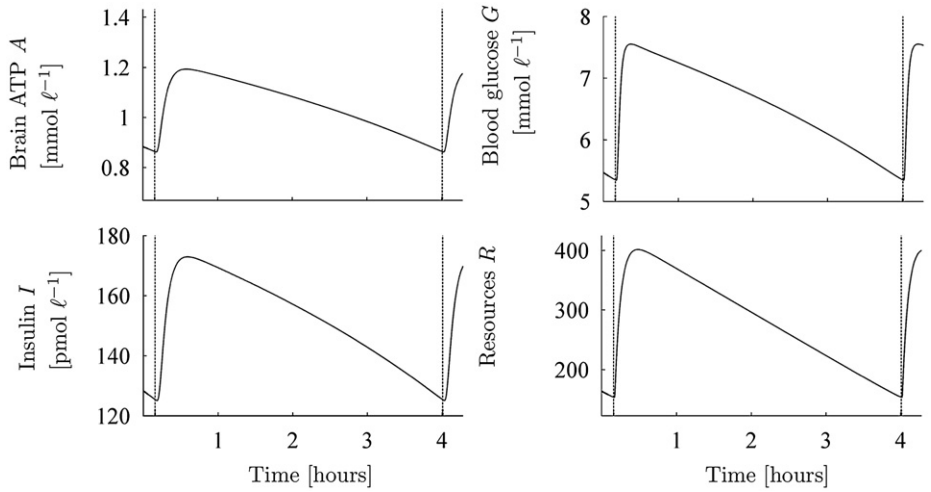

Fig. 3. Brain ATP *A*, blood glucose *G*, insulin *I*, and energy resources in the body *R* without intervention simulated by model (2). The concentrations increase after food intake (vertical lines) and decrease due to the energy consumption of the organism.

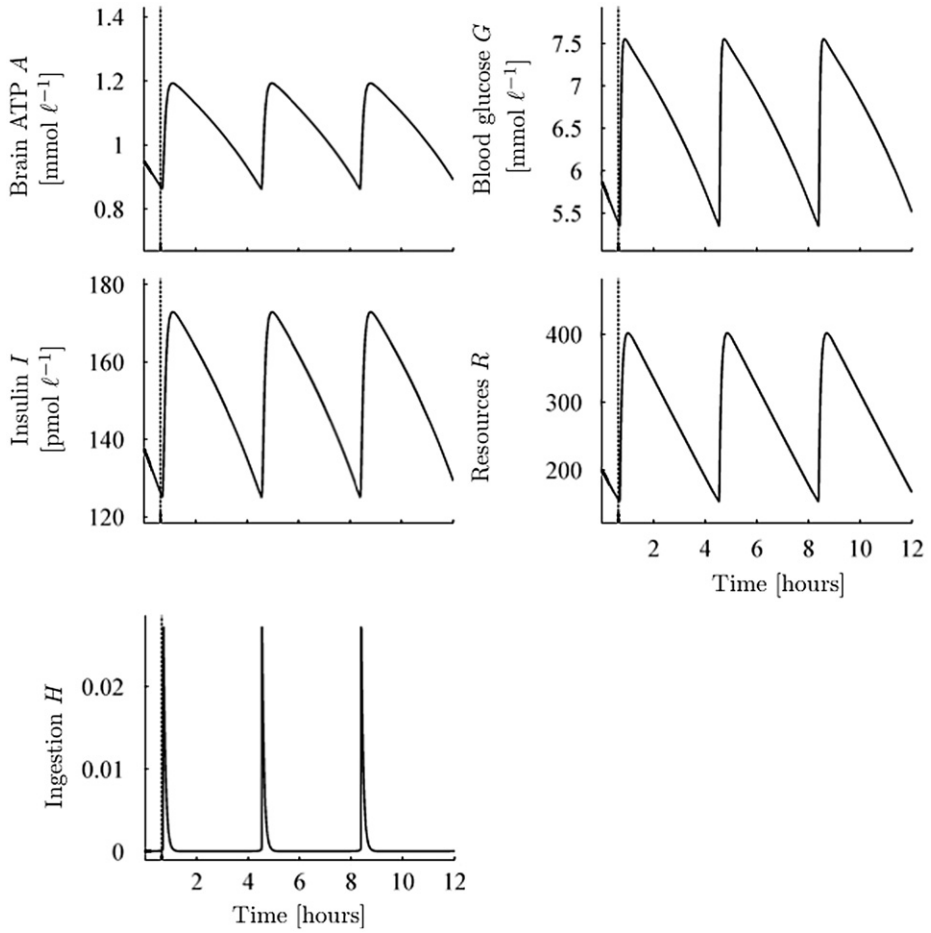

Fig. 4. Brain ATP *A*, blood glucose *G*, insulin *I*, energy resources in the body *R*, and ingestion *H* without intervention simulated with model (2). Modeling the appetite regulation on a short time scale yields cyclic ingestive behavior and thus oscillating concentrations in the compartments. After food intake the concentrations increase and they decrease due to the energy consumption of the organism.

4.1. The energy metabolism at rest

Simulations with system (2) show periodic ingestive behavior and oscillating concentrations in all compartments (compare Fig. 3 for a detailed view and Fig. 4 in the Appendix). The simulation results reflect both mechanisms to provide the brain with sufficient energy, allocation and ingestion. When the brain ATP level *A* decreases, the brain first protects its energy supply via allocation. The insulin concentration *I* drops in order to reduce the glucose uptake into the resources and to strengthen the glucose

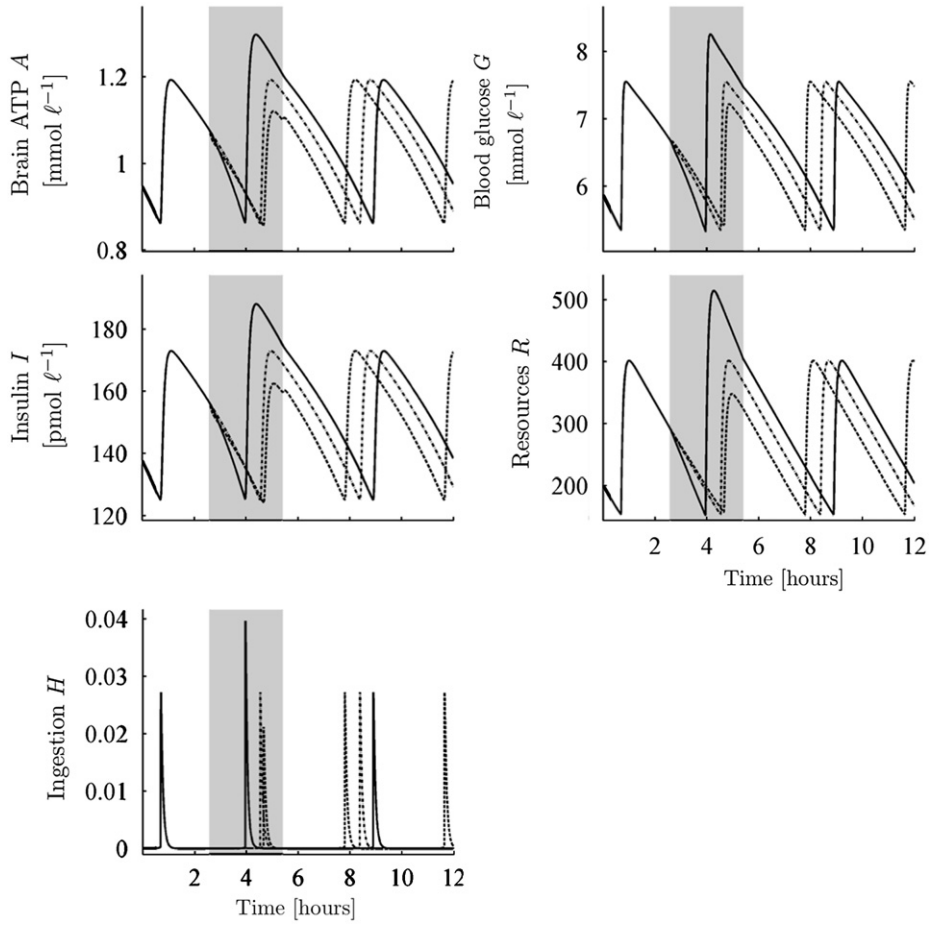

Fig. 5. Brain ATP A, blood glucose G, insulin I, energy resources in the body R, and ingestion H with physical exercise (solid) and during exhaustion (dashed) compared to the simulation results without interventions (dash-dot). Shown are the simulation results of model (2) with the function f (11). During exercise the peripheral energy consumption c_2 is increased by 50% whereas during exhaustion the brain energy consumption c_1 is increased by 2% and the peripheral energy consumption c_2 is reduced by 10% (gray background).

flow across the blood brain barrier from the blood into the brain. The available blood glucose is assimilated into the brain since the glucose flux across the blood brain barrier is insulin independent. By the time, the blood glucose content G additionally decreases, the allocation mechanism is not sufficient to adequately supply the brain with energy so that the appetite additionally rises. The food intake H increases and food is ingested. Hereafter, the energy levels R, G, and A increase, first the energy resources R (at $t \approx 0.692$ h, see Fig. 3) as it includes the gastrointestinal tract. Following, the ingested energy attains to the blood ($t \approx 0.695$ h) and to the brain ($t \approx 0.700$ h). Finally, the insulin concentration I increases ($t \approx 0.706$ h) since the hormone is required to abolish excess glucose from the blood. Thus, the model (2) reproduces the physiological periodic appetite generation due to social or natural cycling (Langemann and Peters, 2008) generating oscillating energy levels in the compartments.

In the course of the day, the blood glucose concentration varies from about 5.3 to 7.5 mmol/ℓ whereas the insulin concentration lies between 120 and 180 pmol/ℓ (Day et al., 2003). With these blood glucose concentrations the brain ATP level is about 0.9–1.2 mmol/ℓ (Ainscow et al., 2002). According to Day et al. (2003) it takes about 18 min for glucose and 26 min for insulin to reach the maximum concentration after meal. In our simulations, the maxima are reached after 11.6 and 25.2 min, respectively. The simulation results of model (2) show a realistic behavior of the circadian rhythm of the healthy human whole body energy metabolism at rest.

Long-term effects in the energy metabolism are simulated by model (12). The unique stationary point $(A_\infty, G_\infty, I_\infty, R_\infty)^\top \approx (0.74, 4.62, 107.24, 100.91)^\top$ of system (12) is asymptotically stable since the chosen parameter values fulfill the conditions (10). In the simulation results, we observe stable energy levels (compare Fig. 6 before the intervention interval). This can be interpreted as the energy metabolism is homeostatically regulated on a long time scale.

4.2. The energy metabolism upon exercise

Here, we discuss a long-term load as it exemplarily occurs with a marathon. During physical exercise more energy is consumed by the organism, particularly by the muscle tissue. In our mathematical model, this intervention can be modeled by a temporary increase in peripheral energy consumption c_2.

With our model (2) we observe an increased food intake with the long-term load and stronger oscillations in all compartments (compare solid lines in Fig. 5). Compared to the resting state (dash-dotted lines) the energy levels increase to a bigger extent. Furthermore, more energy is consumed by the body during exercise so that the energy levels drop.

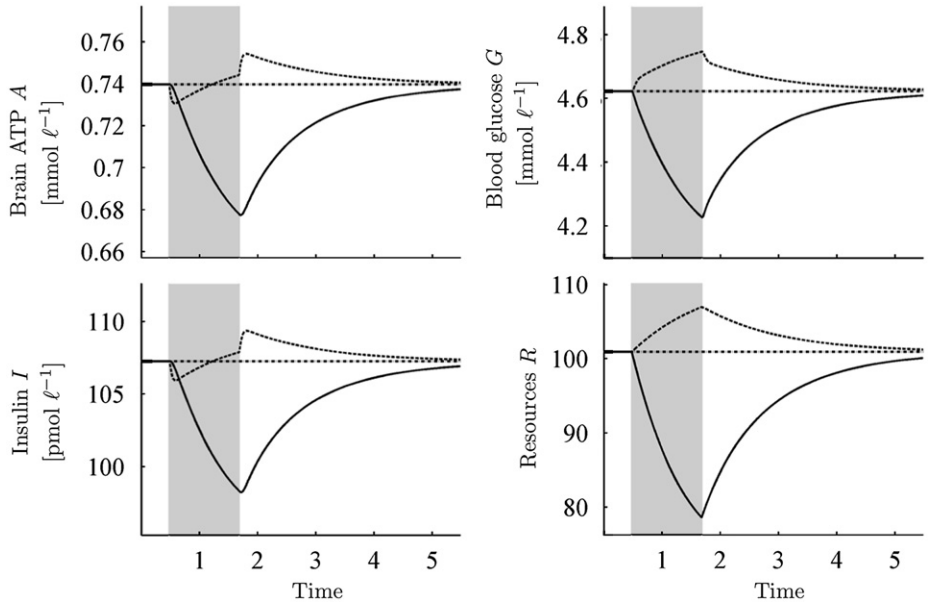

Fig. 6. Brain ATP A, blood glucose G, insulin I, and energy resources in the body R with physical exercise (solid) and during exhaustion (dashed) compared to the simulation results without interventions (dash-dot). Shown are the simulation results of model (12) with $p_6 f(V) = V$, which describes effects on a long time scale. During exercise the peripheral energy consumption c_2 is increased by 50% whereas during exhaustion the cerebral energy consumption c_1 is increased by 2% and the peripheral energy consumption c_2 is reduced by 10%. The gray background marks the intervention interval.

In order to assure the energy supply of the organism during a long-term load more energy is ingested, and food intake occurs more frequently. Thus, the ingested energy increases the resources in the body, and more glucose is available in the blood to satisfy the energy demand. Compared to the resting state the brain ATP level increases as well. The energy flux across the blood brain barrier slightly increases as the blood glucose concentration is elevated while the energy demand of the brain remains stable. Compared to the resting state the insulin concentration increases since the brain is not lacking energy, and the available energy is allocated to the periphery especially to the muscles.

Regarding the long-term effects with system (12) we observe that increased peripheral energy consumption c_2 causes decreased energy levels A, G, and R as well as reduced insulin concentration I on a long time scale (compare solid lines in Fig. 6). During physical exhaustion more energy is consumed, which reduces the energy resources in the body R, the blood glucose concentration G, and slightly the brain ATP level A. The lower brain energy content A activates the allocation via reduction of the insulin level I to assure the energy supply of the brain.

4.3. The energy metabolism upon exhaustion

In this subsection, we discuss exhaustion as it exemplarily occurs during hypoxia. In our model, this intervention can be interpreted as temporary increase in brain energy consumption c_1 and reduced peripheral energy consumption c_1. A transient increase in cerebral activity due to hypoxia has been observed experimentally (Inoue et al., 2004).

Our simulations with model (2) upon exhaustion are shown in Fig. 5 (dashed lines). Compared to the resting state (dash-dotted lines) we observe a decreased ingestion H. Hence, less energy flows into the resources R and the blood G. The cerebral ATP level A slightly decreases compared to the resting state since more energy is consumed by the brain due to cerebral activity. The insulin concentration I decreases, too, so that the available energy is allocated to the brain.

Now, we regard the long-term effects with our model (12). Fig. 6 shows the simulation results during exhaustion (dashed lines) in comparison to the resting state (dash-dotted lines). After onset of the intervention, the brain ATP level A first decreases before it increases above its value at rest. A transient increase followed by a gradual decrease in cerebral activity has been observed experimentally during hypoxia (Inoue et al., 2004), what corresponds to our simulation results. But so far it is unknown how the brain ATP level reacts to hypoxia. After the intervention, the cerebral energy consumption returns to the normal value, what leads to a slight increase in the brain ATP level. The insulin concentration I reacts in the same manner in order to assure the brain energy supply via allocation. The blood glucose concentration G quickly rises after onset of the intervention caused by the reduced peripheral energy consumption, and it returns to the normal value after the intervention. This simulation result is supported by the experimental observation that exhaustion induced by hypoxia causes reduced glucose infusion rates in euglycemic clamp experiments (Oltmanns et al., 2004). Caused by the reduced peripheral energy consumption we observe rising energy resources in the body R compared to the level at rest as well.

5. Discussion and conclusion

We presented an autonomous dynamical system describing the human energy metabolism including the brain not only as consumer but also as superior administrative instance in the regulatory system. The mathematical model describes the brain ATP level, the blood glucose concentration, and the peripheral energy combining fat, muscles, liver, and gastrointestinal tract. The hormone insulin is regarded as feedback signal of the brain. Furthermore, the allocation mechanism and the ingestion regulation are included in the model. These mechanisms provide the brain with sufficient energy.

Generally, mathematical models of the energy metabolism base on theoretical principles. One fundamental principle is the

energy transfer balance, which is achieved with the described model. In our model, we add the competition for energy resources mainly between brain and periphery and the priority of the brain energy supply. Brain ATP plays a decisive role in our mathematical model. The allocation of energy resources within the body mediated via the insulin concentration as well as the appetite are mainly regulated by the brain energy content. Thus, our model comprises the central role of the brain in regulating the energy metabolism, interpreted as the priority of the brain energy supply in the principle of competition for energy resources.

The simulation results show a realistic qualitative behavior of the energy metabolism. Modeling the appetite regulation on a short time scale yields the physiological periodic food intake and oscillating energy levels in the compartments. Therefore, the model describes the circadian ingestive behavior with the typical blood glucose and insulin variations. However, examining a mean ingestion on a long time scale results in stable, respectively, homeostatic energy levels. Additionally, our model realistically reflects certain scenarios such as exercise and exhaustion. The presented brain centered energy metabolism model including the two central roles of the brain is a step into a systemic understanding of the human energy metabolism, and therefore it may give insight into pathological pathways.

In forthcoming investigations, we want to examine the presented model behavior dealing with certain medical interventions such as glucose tolerance tests. A sensitivity analysis of the model parameters will be conducted with our model. Comparing the model with medical data may result in new insights and understanding of the energy metabolism. Imbalances in the energy metabolism lead to metabolic diseases like obesity, anorexia, and type 2 diabetes mellitus. These pathologies feature certain disease patterns, but the origins are fairly unknown. Their symptoms suggest the influence of certain model parameters, which can be interpreted as possible cause of the disease. Additionally, our model shall be expanded by further compartments, and it shall be discussed in its interactions to other regulatory systems as the stress axis (Conrad et al., 2009) and memory (Langemann et al., 2008).

Acknowledgements

This work was supported by the Computational Life Science Initiative at Emory University and by the Graduate School for Computing in Medicine and Life Sciences funded by the German Research Foundation.

Appendix A. Detail appendix for the proof of Theorem 3.4

The coefficients of the characteristic polynomial (9) are given by

$$a_4 = 1,$$

$$a_3 = \frac{p_3 + c_1(2 + c_1 + A_\infty + 2p_4A_\infty^2)}{c_1A_\infty},$$

$$a_2 = \frac{c_1^2 + c_1p_3 + p_3 + A_\infty(c_1^2 + 2c_1 + p_3) + 2c_1^2p_4A_\infty^2 + p_4A_\infty^3(2c_1 - p_3g')}{c_1A_\infty^2},$$

$$a_1 = 3p_4c_1 + \frac{p_3 + c_1 + \frac{p_3}{c_1}}{A_\infty^2} - p_3p_4g'\left(2 + \frac{A_\infty}{c_1}\right),$$

$$a_0 = -3p_3p_4g'.$$

The Hurwitz determinates $\mathcal{H}_2$ and $\mathcal{H}_3$ in $g' = 0$ read

$$\begin{aligned}\mathcal{H}_2(0) = {} & (c_1^2A_\infty^3)^{-1}(c_1^4 + 4p_3c_1^2 + p_3^2 + c_1^3(2 + p_3) + p_3c_1(2 + p_3) \\ & + A_\infty(2c_1 + c_1^2 + p_3)^2 + p_4c_1A_\infty^3(8c_1 + 3c_1^2 + 4p_3) + 4c_1^2p_4^2A_\infty^5 \\ & + 2c_1^2p_4A_\infty^4(1 + 2c_1p_4) + c_1A_\infty^2(p_3 + 2c_1^3p_4 + 2p_3p_4 + c_1^2(1 + 6p_4) \\ & + c_1(2 + 4p_3p_4))),\end{aligned}$$

$$\begin{aligned}\mathcal{H}_3(0) = {} & (c_1^3A_\infty^5)^{-1}(A_\infty(2c_1 + c_1^2 + p_3)^2(c_1^2 + p_3 + c_1p_3) + (2c_1 + c_1^2 \\ & + p_3)(c_1^2 + p_3 + c_1p_3)^2 + c_1p_4A_\infty^3(15c_1^4 + 3c_1^5 + 27c_1^2p_3 + 4p_3^2 \\ & + c_1p_3(8 + 7p_3) + c_1^3(20 + 9p_3)) + c_1^2p_4^2A_\infty^5(28c_1^2 + 9c_1^3 + 4p_3 \\ & + 16c_1p_3) + 12c_1^4p_4^3A_\infty^7 + 6c_1^4p_4^2A_\infty^6(1 + 2c_1p_4) \\ & + c_1^2p_4A_\infty^4(2p_3 + 6c_1^4p_4 + c_1^3(3 + 22p_4) + 8c_1^2(1 + 2p_3p_4) \\ & + 5c_1(p_3 + 2p_3p_4)) + c_1A_\infty^2(c_1^2 + p_3 + c_1p_3)(p_3 + 5c_1^3p_4 + 2p_3p_4 \\ & + c_1^2(1 + 12p_4) + c_1(2 + 7p_3p_4))),\end{aligned}$$

with its first derivatives in $g' = 0$

$$\mathcal{H}_2'(0) = p_3p_4\left(1 - \frac{2}{c_1} - \frac{p_3}{c_1^2} - 2\frac{p_4}{c_1}A_\infty^2\right),$$

$$\begin{aligned}\mathcal{H}_3'(0) = {} & -(c_1^3A_\infty^3)^{-1}(p_3p_4(2c_1(c_1^4 + 4c_1^2p_3 + p_3^2 + c_1^3(2 + p_3) \\ & + c_1p_3(2 + p_3)) + A_\infty(-4c_1^4 - c_1^5 + 2c_1^2p_3 - 2c_1^3p_3 + 2p_3^2 \\ & + c_1p_3(4 + p_3)) + 4c_1^2p_4^2A_\infty^6 + 2c_1^2p_4A_\infty^5(1 + 3c_1p_4) \\ & + c_1p_4A_\infty^4(8c_1 - 5c_1^2 + 4p_3 + 8c_1^3p_4) + c_1A_\infty^3(p_3 - 7c_1^3p_4 + 4p_3p_4 \\ & + c_1^2(-2 + 6p_4) + c_1(2 + 5p_3p_4)) + A_\infty^2(4c_1p_3 + p_3^2 + 4c_1^5p_4 \\ & + 3c_1^4(-1 + 4p_4) + c_1^2(4 - 2p_3 + 4p_3p_4) + c_1^3(-4 + 8p_3p_4)))),\end{aligned}$$

and the second derivative of $\mathcal{H}_3$ in $g' = 0$ is given by

$$\mathcal{H}_3''(0) = c_1^{-3}(2p_3^2p_4^2(A_\infty + 2c_1)(-c_1^2 + p_3 + 2c_1(1 + p_4A_\infty^2))).$$

Appendix B. Appendix for the numerical simulations in Section 4

The numerical simulations on a long time scale with the system (7) were done with the non-scaled system in order to obtain physiological values. We choose $p_6f(V) = V$ and then the non-scaled system (7) reads

$$\dot{A} = p_1\frac{G}{A} - c_1, \tag{12a}$$

$$\dot{G} = -p_1\frac{G}{A} - p_2GI + p_3\frac{R}{G}, \tag{12b}$$

$$\dot{I} = p_4A - p_5I, \tag{12c}$$

$$\dot{R} = p_2GI - p_3\frac{R}{G} + \frac{p_8}{AGI} - c_2, \tag{12d}$$

with the unique stationary point

$$(A_\infty, G_\infty, I_\infty, R_\infty)^\top = \left(\sqrt[3]{\frac{p_1p_5p_8}{c_1cp_4}}, \frac{c_1}{p_1}A_\infty, \frac{p_4}{p_5}A_\infty, \frac{c_1^2A_\infty}{p_1p_3}\left(1 + \frac{p_2p_4}{p_1p_5}A_\infty^2\right)\right)^\top.$$

References

Ackerman, E., 1964. A mathematical model of the glucose-tolerance test. Phys. Med. Biol. 9 (2), 203–213.

Ainscow, E.K., Mirshamsi, S., Tang, T., Ashford, M.L.J., Rutter, G.A., 2002. Dynamic imaging of free cytosolic ATP concentration during fuel sensing by rat hypothalamic neurones: evidence for ATP-independent control of ATP-sensitive K(+) channels. J. Physiol. 544 (Pt 2), 429–445.

Baron, A.D., Clark, M.G., 1997. Role of blood flow in the regulation of muscle glucose uptake. Annu. Rev. Nutr. 17, 487–499.

Bergman, R., Phillips, L., Cobelli, C., 1981. Physiologic evaluation of factors controlling glucose tolerance in man: measurement of insulin sensitivity and beta-cell glucose sensitivity from the response to intravenous glucose. J. Clin. Invest. 68 (6), 1456–1467.

Clark, D.D., Sokoloff, L., 1999. In: Siegel, G.J., Agranoff, B.W., Albers, R.W., Fisher, S.K., Uhler, M.D. (Eds.), Basic Neurochemistry: Molecular, Cellular and Medical Aspects. Elsevier Academic Press, San Diego, pp. 637–670.

Conrad, M., Hubold, C., Fischer, B., Peters, A., 2009. Modeling the hypothalamus–pituitary–adrenal system: homeostasis by interacting positive and negative feedback. J. Biol. Phys. 35, 149–162.

Day, C., Archer, H., Bailey, C.J., 2003. Recent advances in insulin therapy. Br. J. Cardiol. 10, 379–383.

Flakoll, P.J., Wentzel, L.S., Rice, D.E., Hill, J.O., Abumrad, N.N., 1992. Short-term regulation of insulin-mediated glucose utilization in four-day fasted human volunteers: role of amino acid availability. Diabetologia 35 (4), 357–366.

Fugleberg, S., Kolendorf, K., Thorsteinsson, B., Bliddal, H., Lund, B., Bojsen, F., 1982. The relationship between plasma concentration and plasma disappearance rate of immunoreactive insulin in normal subjects. Diabetologia 22 (6), 437–440.

Inoue, S., Yamanaka, T., Okamoto, H., Hosoi, H., 2004. Effect of a glutamate blocker, ipenoxazone hydrochloride on the hypoxia-induced firing in the medial vestibular nucleus. Acta Otolaryngol Suppl. 553, 58–60.

Kennedy, G., 1953. The role of depot fat in the hypothalamic control of food intake in the rat. Proc. R. Soc. London B Biol. Sci. 140 (901), 578–592.

Khalil, H.K., 2002. Nonlinear Systems, third ed. Pearson Higher Education, New Jersey.

Langemann, D., 2007. Selfish brain theory: mathematical challenges in the top-down analysis of metabolic supply chains. In: Grundy, J. (Ed.) Proceedings of the Tutorials, Posters, Panels and Industrial Contributions at the 26th International Conference on Conceptual Modeling—ER 2007 Auckland, New Zealand, CRPIT, vol. 83, pp. 39–49.

Langemann, D., Pellerin, L., Peters, A., 2008. Making sense of AMPA receptor trafficking by modeling molecular mechanisms of synaptic plasticity. Brain Res. 1207, 60–72.

Langemann, D., Peters, A., 2008. Deductive functional assignment of elements in appetite regulation. J. Biol. Phys. 34, 413–424.

Marty, N., Dallaporta, M., Thorens, B., 2007. Brain glucose sensing, counter-regulation, and energy homeostasis. Physiology 22, 241–251.

Mayer, J., 1953. Glucostatic mechanism of regulation of food intake. N. Engl. J. Med. 249 (1), 13–16.

Oltmanns, K.M., Gehring, H., Rudolf, S., Schultes, B., Rook, S., Schweiger, U., Born, J., Fehm, H.L., Peters, A., 2004. Hypoxia causes glucose intolerance in humans. Am. J. Respir. Crit. Care. Med. 169 (11), 1231–1237.

Öz, G., Kumar, A., Rao, J.P., Kodl, C.T., Chow, L., Eberly, L.E., Seaquist, E.R., 2009. Human brain glycogen metabolism during and after hypoglycemia. Diabetes 58 (9), 1978–1985.

Peters, A., Conrad, M., Hubold, C., Schweiger, U., Fischer, B., Fehm, H.L., 2007a. The principle of homeostasis in the hypothalamus-pituitary-adrenal system: new insight from positive feedback. Am. J. Physiol. Regul. Integr. Comput. Physiol. 293 (1), R83–R98.

Peters, A., Pellerin, L., Dallman, M.F., Oltmanns, K.M., Schweiger, U., Born, J., Fehm, H.L., 2007b. Causes of obesity: looking beyond the hypothalamus. Prog. Neurobiol. 81 (2), 61–88.

Peters, A., Schweiger, U., Pellerin, L., Hubold, C., Oltmanns, K.M., Conrad, M., Schultes, B., Born, J., Fehm, H.L., 2004. The selfish brain: competition for energy resources. Neurosci. Biobehav. Rev. 28 (2), 143–180.

Simon, C., Weibel, L., Brandenberger, G., 2000. Twenty-four-hour rhythms of plasma glucose and insulin secretion rate in regular night workers. Am. J. Physiol. Endocrinol. Metab. 278 (3), E413–E420.

Tsuji, A., 2005. Small molecular drug transfer across the blood-brain barrier via carrier-mediated transport systems. NeuroRx 2 (1), 54–62.

Vatov, L., Kizner, Z., Ruppin, E., Meilin, S., Manor, T., Mayevsky, A., 2006. Modeling brain energy metabolism and function: a multiparametric monitoring approach. Bull. Math. Biol. 68 (2), 275–291.

Walter, W., 1970. Differential and Integral Inequalities. Springer, Berlin.

Wang, P., Mariman, E.C.M., 2008. Insulin resistance in an energy-centered perspective. Physiol. Behav. 94 (2), 198–205.